

Reconstitution *in vitro* of the entire cycle of the mouse female germ line

Orie Hikabe^{1*}, Nobuhiko Hamazaki¹, Go Nagamatsu¹, Yayoi Obata², Yuji Hirao³, Norio Hamada^{1,4}, So Shimamoto¹, Takuya Imamura¹, Kinichi Nakashima¹, Mitinori Saitou^{5,6,7,8} & Katsuhiko Hayashi^{1,9*}

The female germ line undergoes a unique sequence of differentiation processes that confers totipotency to the egg^{1,2}. The reconstitution of these events *in vitro* using pluripotent stem cells is a key achievement in reproductive biology and regenerative medicine. Here we report successful reconstitution *in vitro* of the entire process of oogenesis from mouse pluripotent stem cells. Fully potent mature oocytes were generated in culture from embryonic stem cells and from induced pluripotent stem cells derived from both embryonic fibroblasts and adult tail tip fibroblasts. Moreover, pluripotent stem cell lines were re-derived from the eggs that were generated *in vitro*, thereby reconstituting the full female germline cycle in a dish. This culture system will provide a platform for elucidating the molecular mechanisms underlying totipotency and the production of oocytes of other mammalian species in culture.

One of the key goals in developmental and reproductive biology is to reconstitute the entire process of gametogenesis in culture. Specifically, owing to its biological significance, reconstitution of oogenesis using pluripotent stem cells that yields functional eggs has long been sought^{3–5}. Eggs originate from primordial germ cells (PGCs), which are specified at around embryonic day 6.5 (E6.5) in mice⁶. PGCs then migrate into the gonads, enter meiosis in female embryos⁷, and therefore become primary oocytes. Following puberty, primary oocytes begin to grow to mature oocytes that are fully ready for fertilization. We previously reported a culture system in which mouse pluripotent stem cells differentiated into PGC-like cells (PGCLCs) that were capable of differentiating into functional oocytes by transplantation into immunocompromised female mice⁸. However, this system recapitulates a quite short window of embryogenesis, from the blastocyst to migratory PGC stage, requiring only 4 to 5 days *in vivo*. There thus remains a long period of time (perhaps over a month) that must be reconstituted to produce mature oocytes in culture.

To reconstitute the entire process of oogenesis *in vitro*, the culture period was divided into three sections in this study: (1) *in vitro* differentiation (IVDi), (2) *in vitro* growth (IVG) and (3) *in vitro* maturation (IVM), in which oogenesis would proceed to primary oocytes in the secondary follicle, fully grown germinal vesicle oocytes and metaphase II (MII) oocytes, respectively (Fig. 1a). As we reported previously⁸, PGCLCs differentiated from a female embryonic stem cell (ESC) line, BVSC18 (129^{+/Ter}/svj (agouti) × C57BL/6), that harbours *Blimp1-mVenus* (BV) and *stella-EGFP* (SC) reporter constructs, were aggregated with E12.5 female gonadal somatic cells of albino ICR strain. In IVDi, the aggregates, hereafter called reconstituted ovaries (rOvaries), were placed on Transwell-COL, a culture insert coated with collagen, and soaked with α MEM-based medium. At 4 days of culture, the medium was replaced with StemPro34-based medium, as

the combination of media yielded a high number of primary oocytes with a follicle structure in preliminary culture experiments (Extended Data Fig. 1a). To prevent multiple oocyte follicle formation such as that seen frequently in culture (Extended Data Fig. 1b), we added the oestrogen inhibitor ICI182780 to the culture⁹. The rOvaries were filled throughout with follicle structures, each of which possesses a single oocyte, in an ICI182780-dependent manner (Extended Data Fig. 1b, c). During IVDi culture, BV, a marker of early PGCs¹⁰, was detectable at 3 days of culture, but became weak after one week of culture (Fig. 1b). At two weeks of culture, BV disappeared and SC—a marker of both oocytes and PGCs—became prominent in rOvaries, and at three weeks of culture, a number of SC-positive primary oocytes were observed in rOvaries (Fig. 1b). The close observation of IVDi revealed that clusters of PGCLCs were formed by 5 days of culture and gradually fragmented from 5 to 9 days, after which, follicles were formed around 11 days of culture (Extended Data Fig. 2a). FoxL2, a functional marker of granulosa cells, was detectable in cells surrounding the oocytes at 21 days of culture (Extended Data Fig. 2a). Immunofluorescence analysis of the meiotic chromosome revealed the robust progression of meiotic prophase I from 5 to 9 days of culture (Extended Data Fig. 2b, c). PGCLCs before aggregation are equivalent to E9.5 (refs 8, 11). Therefore, the meiotic prophase I in PGCLCs progresses during the period corresponding to E14.5 (E9.5 + 5 days) through to E18.5 (E9.5 + 9 days), which is also seen in meiotic prophase I in fetal ovaries *in vivo*¹². At the pachytene stage, however, asynapsis between homologous chromosomes occurred more frequently *in vitro* (53.8%) than *in vivo* (5.3%) (Extended Data Fig. 2d). This was partially due to culture *in vitro*, as the percentage increased even in primary oocytes in the organ culture of gonads under the same condition (Extended Data Fig. 2d). Although chromosome pairing *in vitro* was not as accurate as that *in vivo*, IVDi culture yielded a large number of secondary follicle-like structures (2FLs) at three weeks of culture; on average ($n = 8$), 237.3 ± 27.3 2FLs were formed per rOvary. SC-negative residual oocytes were sparsely scattered in the rOvaries (Fig. 1b, Extended Data Fig. 1c); the percentage of SC-negative oocytes was $4.4 \pm 2.1\%$ (the mean \pm s.d., $n = 4$, 3163 oocytes in total). These results demonstrated that a robust number of primary oocytes were induced from ESCs under the culture conditions employed.

Oocyte growth accompanied with follicular growth is tightly controlled by gonadotropins². Follicle-stimulating hormone plays a central role in the proliferation and maturation of granulosa cells. In culture with IVG medium that contains follicle-stimulating hormone, however, proliferation of the granulosa cell layer was limited in 2FLs located at the edge of the rOvary (Extended Data Fig. 3a), suggesting that 2FLs in the centre portion lack signalling and/or space for cell growth. Therefore, individual 2FLs were manually separated from the

¹Department of Stem Cell Biology and Medicine, Graduate School of Medical Sciences, Kyushu University, Maidashi 3-1-1, Higashi-ku, Fukuoka 812-8582, Japan. ²Department of Bioscience, Tokyo University of Agriculture, 1-1-1, Sakuragaoka, Setagaya-ku, Tokyo 156-8502, Japan. ³NARO Institute of Livestock and Grassland Science, Ikenodai 2, Tsukuba 305-0901, Japan. ⁴Department of Obstetrics and Gynecology, Graduate School of Medical Sciences, Kyushu University, Maidashi 3-1-1, Higashi-ku, Fukuoka 812-8582, Japan. ⁵Department of Anatomy and Cell Biology, Graduate School of Medicine, Kyoto University, Yoshida-Konoe-cho, Sakyo-ku, Kyoto 606-8501, Japan. ⁶Center for iPS Cell Research and Application, Kyoto University, 53 Kawahara-cho, Shogoin, Sakyo-ku, Kyoto 606-8507, Japan. ⁷Institute for Integrated Cell-Material Sciences, Kyoto University, Yoshida-Ushinomiya-cho, Sakyo-ku, Kyoto 606-8501, Japan. ⁸JST, ERATO, Yoshida-Konoe-cho, Sakyo-ku, Kyoto 606-8501, Japan. ⁹JST, PRESTO, Maidashi 3-1-1, Higashi-ku, Fukuoka 812-8582, Japan.

*These authors contributed equally to this work.

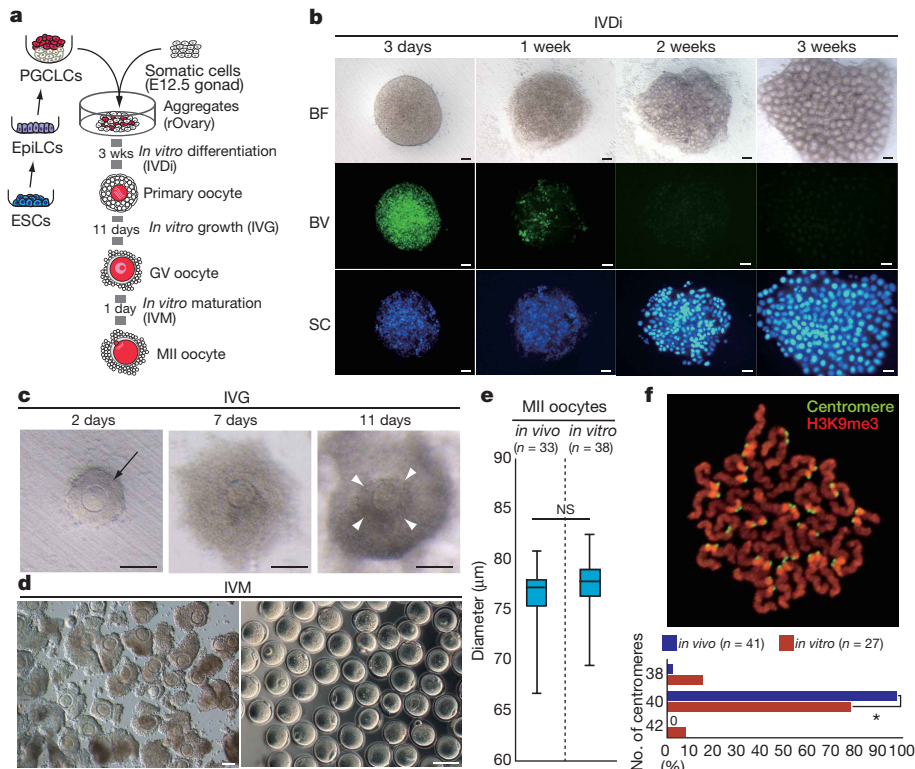


Figure 1 | Oocyte production from pluripotent stem cells. **a**, A schematic of oocyte production *in vitro*. **b**, rOvary during IVDi. A representative rOvary on days indicated are shown. BF, bright field; BV, *Blimp1-mVenus*; SC, *stella-ECFP*. **c**, Follicular growth during IVG. Granulosa cells (black arrow) proliferated and then formed a cumulus–oocyte complex (white arrowheads). **d**, Cumulus–oocyte complexes before IVM (left) and MII oocytes after IVM (right). A large image of the MII oocytes is shown in Extended Data Fig. 3d. **e**, Diameters of the *in-vitro*-generated MII oocytes

rOvaries (Extended Data Fig. 3b). As expected, granulosa cells proliferated and cumulus–oocyte complexes were formed the isolated 2FLs (Fig. 1c). When cultured for 11 days, primary oocytes in 2FLs grew to germinal vesicle oocytes (Fig. 1c). In total, 3,198 fully grown germinal vesicle oocytes were obtained from 58 rOvaries in three culture experiments (Extended Data Fig. 3c); on average, 55.1 fully grown oocytes were obtained from one rOvary. When transferring them under the IVM culture conditions, 28.9% of the germinal vesicle oocytes extruded a 1st polar body (Fig. 1d and Extended Data Fig. 3c, d). The percentage of SC-negative MII oocytes was $4.6 \pm 0.7\%$ (mean \pm s.d., $n = 3,565$ MII oocytes in total), suggesting that the contamination rate of endogenous oocytes remained low. The diameters of SC-positive MII oocytes generated *in vitro* were comparable to those of MII oocytes *in vivo* (Fig. 1e). Consistently, the maternal pattern of DNA methylation in the differentially methylated region (DMR) of imprinted genes, which is established in an oocyte size-specific manner¹³, was almost complete at the representative gene loci tested (*H19* and *Igf2r*) (Extended Data Fig. 3e). The frequency of aneuploidy increased to some extent, but most (77.8%) of the MII oocytes generated *in vitro* had a correct number of chromosomes (Fig. 1f). These results demonstrate that, despite sporadic flaws in some oocytes, a robust number of MII oocytes were produced from pluripotent stem cells in a dish.

To evaluate oogenesis *in vitro*, the global transcription dynamics during the culture were determined by RNA sequencing (RNA-seq) analysis. We used poly(A) RNA from ESCs, PGCLCs before aggregation (PGCLCs-d6), PGCLCs at 3 days of aggregation (PGCLC-agg3), SC-positive primary oocytes in 2FLs (vitro-2nd) and MII oocytes generated *in vitro* (vitro-MII). For comparison, poly(A) RNAs from E12.5 female PGCs (PGCs-E12.5), primary oocytes in secondary follicles in post-natal day 8 (P8) ovaries (vivo-2nd) and MII oocytes

in 2 independent experiments. NS, not significant (*t*-test, $P > 0.05$). **f**, Meiotic chromosome in *in-vitro*-generated MII oocytes in 3 independent experiments. Centromeres (green) and H3K9me3 (red) (upper), and the number of centromeres in the MII oocytes (bottom) are shown. The percentage of *in-vitro*-generated MII oocytes harbouring 40 centromeres was lower (chi-squared test, $*P < 0.05$) than that of MII oocytes *in vivo*. Scale bars in **b**, **c** and **d**, 100 μm .

superovulated from adult ovaries (vivo-MII) were used. Principal component analysis showed that oogenesis *in vitro* largely recapitulated the differentiation process *in vivo* (Fig. 2a). Consistently, the expression dynamics of genes involved in oogenesis was similar to those *in vivo* (Fig. 2b). Repetitive elements, such as long interspersed elements, short interspersed elements and satellite sequences, were repressed in oocytes both *in vitro* and *in vivo*, and the transcripts of long terminal repeat (LTR) transposons was temporarily upregulated in the primary oocytes both *in vivo* and *in vitro* (Extended Data Fig. 4a). Endogenous retrovirus group K (ERVK) and endogenous retrovirus-like and mammalian apparent LTR-retrotransposon (ERVL–MaLR) accounted for most of the abundant LTR transposon transcripts (Extended Data Fig. 4b). Moreover, the retrotransposons LTR 10 (RLTR10) and mouse transcript A (MTA) transcripts were enriched in ERVK and ERVL–MaLR, respectively (Extended Data Fig. 4c, d). These observations are consistent with previous reports that the transcripts of transposons enriched in growing oocytes are tightly related to oocyte-specific transcriptional regulation^{14,15}. Our results therefore indicate that such an oocyte-specific regulation was firmly reconstituted during oogenesis in culture. The correlation coefficient between global transcripts *in vivo* and *in vitro* at each oogenesis stage was more than 0.98 (Fig. 2c). However, careful comparison of the transcriptome identified differentially expressed genes (DEGs) between oogenesis *in vivo* and *in vitro*. The numbers of DEGs with >4-fold change were 6 and 27 at the PGC- and primary-oocyte-stage, respectively, which was a relatively subtle difference (Fig. 2c). In contrast, at the MII-oocyte-stage, 424 genes were detected as the DEGs; 363 and 61 genes were up- and downregulated, respectively (Fig. 2c). Of note, the DEGs upregulated in MII oocytes *in vitro* were the genes whose transcripts were reduced from primary oocytes to MII oocytes *in vivo*,

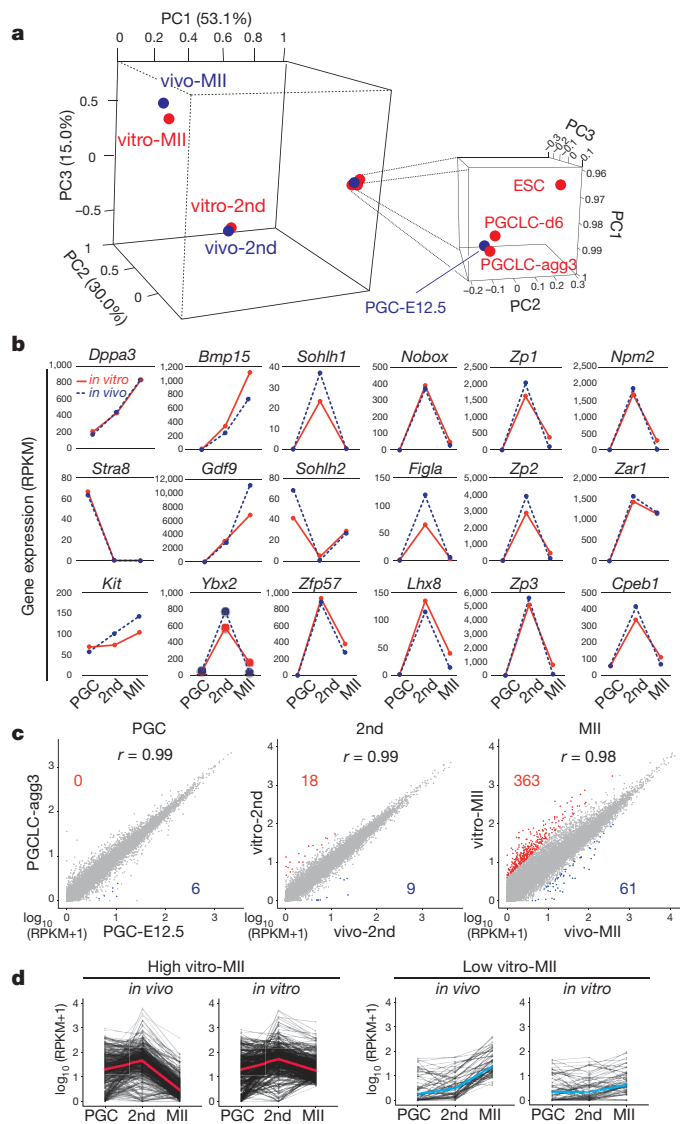


Figure 2 | Transcriptome analysis of oogenesis *in vitro*. **a**, Principal component analysis of each developmental stage. **b**, Gene expression dynamics during oogenesis *in vitro*. RPKMs of gene products in oogenesis *in vitro* (red) and *in vivo* (blue) are shown. PGC on the x axis indicate the comparisons between PGC-agg3 and PGCs-E12.5. **c**, Scatter plot comparison of transcripts between each stage of oogenesis *in vitro* and *in vivo*. Pearson correlation coefficients (r) are shown in the plot. Genes exhibiting more than fourfold higher (red) or fourfold lower (blue) expression *in vitro* than *in vivo* are shown. **d**, Expression dynamics of the DEGs in the MII oocyte stage. The red and blue lines indicate the median values. All expression data are based on the mean values from 3 biological replicates, except for PGC-agg3 that is from 2 biological replicates.

and vice versa: the DEGs downregulated in MII oocytes *in vitro* were the genes whose transcripts were increased from primary oocytes to MII oocytes *in vivo* (Fig. 2d). This indicates that oocyte growth during IVG and IVM culture was compromised in a subset, or perhaps all, of the oocytes. Interestingly, gene ontology analysis illustrated that DEGs upregulated in MII oocytes *in vitro* were related to mitochondrial function (Extended Data Fig. 4e and Supplementary Table 1). Misregulation of these genes might attenuate the potential of MII oocytes generated *in vitro*. Analysis of the metabolic pathway will thus provide information about the refinement of the IVG and IVM culture.

Whether the MII oocytes are capable of developing to offspring is the most stringent criterion for evaluation of the culture system. To test this capability, *in vitro*-generated MII oocytes were subjected to *in vitro* fertilization (IVF) with wild-type sperm of albino ICR strain.

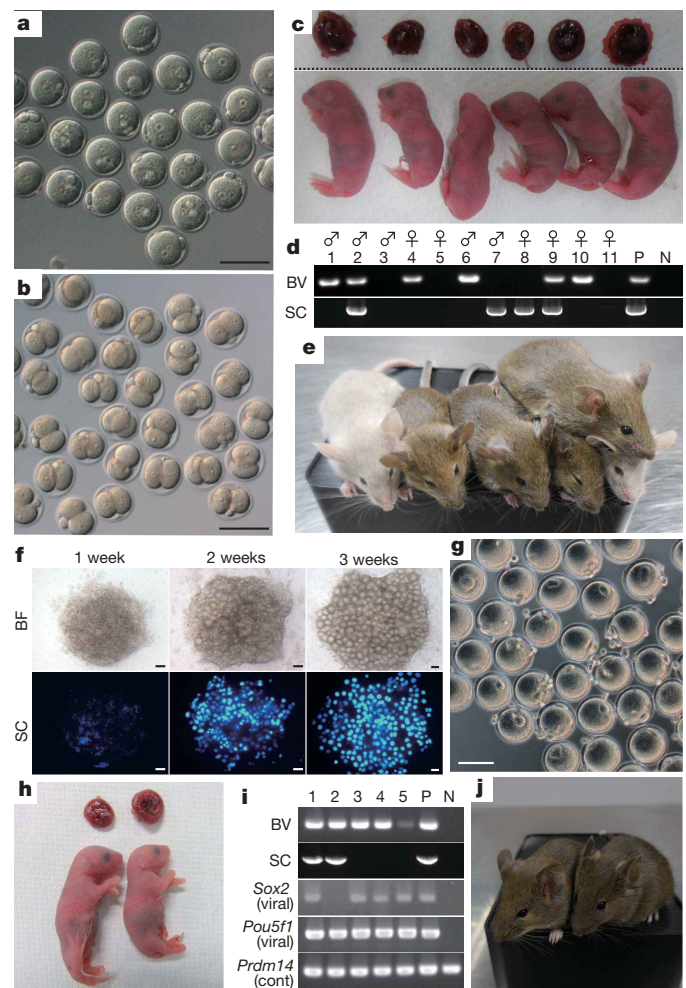


Figure 3 | Offspring from *in vitro*-generated eggs. **a**, Fertilized eggs (**a**) and 2-cell embryos (**b**) from IVF using BVSC18 ESC-derived MII oocytes. **c**, 6 representative pups and their placentas from BVSC18 ESC-derived MII oocytes. **d**, Genotyping by the BV and SC transgenes. **e**, The 6 mice at 4 weeks after birth. **f**, IVDi using TTF-derived iPSCs (TTF4FC6). **g**, MII oocytes from TTF4FC6 after IVM culture. **h**, Two representative pups and their placentas from TTF4FC6-derived MII oocytes. **i**, Genotyping of the pups from TTF4FC6. PCR products from the BV and SC transgenes, exogenous retroviral *Sox2* and *Pou5f1* and the *Prdm14* locus as a positive control for the PCR reaction are shown. **j**, Two mice (from **h**) at 4 weeks after birth. Scale bars, 100 μ m. P, positive control (genomic DNA of a BVSC mouse in **d** and of TTF4FC6 in **i**). N, negative control (genomic DNA of a wild-type mouse). For gel source data see Supplementary Fig. 1.

By IVF, *in vitro*-generated oocytes were fertilized and developed to 2-cell embryos (Fig. 3a, b). 11 (3.5%) out of 316 2-cell embryos transferred to pseudopregnant ICR females were successfully delivered as viable pups with coloured eyes (Fig. 3c, Extended Data Fig. 5a, 5b), showing that the pups were from BVSC18 ESC-derived oocytes, but not from ICR oocytes that could mingle in gonadal somatic cells. The reporter constructs were largely segregated in the expected Mendelian manner (Fig. 3d). The placentas of the pups were heavier than those of wild-type mice (Extended Data Fig. 5c), but this phenomenon was less pronounced than the placentomegaly observed in clone mice¹⁶. In addition, the pups tended to be slightly heavier than the wild-type mice (Extended Data Fig. 5c), which may have been due to the small number (either one or two) of pups in the uterine horn on Caesarean section. Using 2-cell embryos from *in vitro*-generated oocytes, the success rate of full-term development was 3.5%, which is much lower than that from *in vivo*-generated oocytes (61.7%, Extended Data Fig. 6a). A comparison of developmental progression from genetically matched oocytes *in vivo* (129X1/svj \times C57BL/6) demonstrates that the

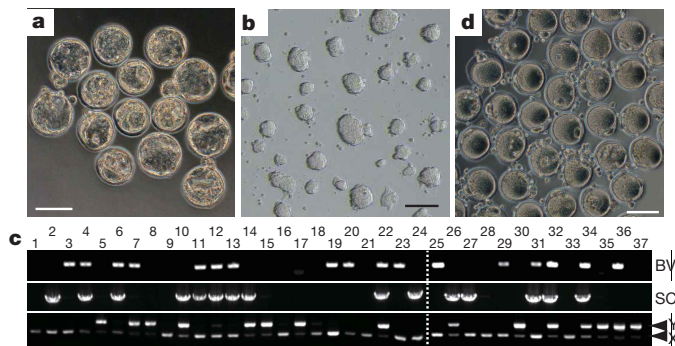


Figure 4 | Reconstitution of the second cycle of oogenesis *in vitro*. **a, b,** Derivation of rESCs. Blastocysts from *in-vitro*-generated eggs (**a**) were used for derivation of rESC (**b**). **c,** Genotyping of rESCs. In total, 37 rESC lines were derived in 2 independent experiments. The BVSC constructs and sex chromosome (X or Y) were determined by PCR. **d,** MII oocytes from rESCs. Scale bars, 100 μ m. For gel source data see Supplementary Fig. 1.

fertilization rates were not significantly different, but embryogenesis was frequently retarded at various stages, such as the cleavage stage, and early and late gestation (Extended Data Fig. 6b–e). The developmental arrest may have been at least partly attributable to aneuploidy (Fig. 1f) and aberrant gene expression (Fig. 2c, d). Nevertheless, the successful production of pups demonstrates that the culture system fulfills the condition of producing functional eggs. Importantly, all of the obtained pups grew up normally without evidence of premature death (Fig. 3e, Extended Data Fig. 5c). Combined bisulfite restriction analysis (COBRA) and bisulfite sequencing of the DMRs revealed that the epigenetic status of the imprinted loci was maintained in a manner comparable to that of wild-type mice (Extended Data Fig. 5d, e). Both females and males from *in-vitro*-generated oocytes were fertile (Extended Data Fig. 5f) and remained alive for at least 11 months without any apparent abnormality (Extended Data Fig. 5g).

To verify the robustness and reproducibility of the culture system, we induced oogenesis in five cell lines *in vitro*: BVSCH14, which is another ESC line of the same mouse strain as BVSCH18, two induced pluripotent stem cell (iPSC) lines from mouse embryonic fibroblasts (MEFs) and two iPSC lines from 10-week-old adult tail tip fibroblasts (TTFs). BVSCH14 and the two MEF-derived iPSC lines (MEF4FRC9 and MEF4FC14) gave rise to a number of oocytes (Extended Data Fig. 7a, Extended Data Table 1). They contained fully potent oocytes, as pups with coloured eyes were obtained from oocytes from each cell line (Extended Data Figs 7a, 8a, b, Extended Data Table 1). The weights of their placentas and bodies showed a similar trend as seen in BVSCH18 (Extended Data Fig. 7b). The reporter genes and retrovirus-derived exogenous genes for the reprogramming were detectable in the pups, as expected (Extended Data Figs 7c, d, 8a, b). All of the pups grew up normally without evidence of premature death. Notably, fully potent oocytes were also generated from the two TTF-derived iPSC lines (TTF4FC6 and TTF4FRC3) (Fig. 3f, g, Extended Data Table 1). Upon fertilization with sperm from ICR males followed by transfer to surrogate mothers, they gave rise to healthy pups with the retroviral genes and the reporter constructs or coloured eyes (Fig. 3h, i, Extended Data Fig. 7d, 7e, 8c, Extended Data Table 1). The weights of the placentas were varied, and some of them were comparable to wild-type placenta (Extended Data Fig. 7b). Although 2 pups were cannibalized by the nursing mother at the day of birth, the remaining 6 pups grew without any apparent abnormality such as tumour formation or developmental arrest (Fig. 3j). Both females and males from iPSC-derived oocytes were fertile (Extended Data Fig. 8d).

Finally, blastocysts from *in-vitro*-generated oocytes were used to derive ESCs, thereby realizing the reconstitution of an entire cycle of the female germ line. The 51 blastocysts from BVSCH18-derived oocytes were placed on embryonic fibroblasts in culture medium containing

CHIR99021, PD0325901 and leukaemia inhibitory factor (2i+LIF)¹⁷. 72.5% of the blastocysts (37 out of 51) gave rise to ESC lines (Fig. 4a–c), which were designated regenerated ESCs (rESCs). The BVSC reporter genes and sex chromosomes were segregated to each rESC clone in the expected Mendelian manner (Fig. 4c). When the rESCs (clone 6) were injected into wild-type blastocysts, they contributed to multiple tissues, including PGCs of the chimaera embryos (Extended Data Fig. 9a, b). As the success rate of rESC derivation was higher than that of full-term development, it is possible that some rESC lines are not fully competent. A critical comparison of pluripotency, gene expression and epigenetic status between these rESC lines might provide important clues to clarify the heterogeneity in quality of *in-vitro*-generated oocytes. We successfully produced rESC-derived MII oocytes that were undergoing second rounds of meiosis from the initial ESCs (Fig. 4d, Extended Data Fig. 9c). Taken together, these results demonstrated the successful reconstitution of an entire cycle of the female germ line *in vitro* (Extended Data Fig. 9d). One limitation of the reconstitution, however, is that the culture system used gonadal somatic cells that were obtained from the embryos. Requirement of gonadal somatic cells would be a critical point, if human PGCLCs^{18,19} are to be progressed to later stages of gametogenesis. One possible way to overcome this issue would be to derive the gonadal somatic cell-like cells from pluripotent stem cells. Nevertheless, the culture system used here will provide an important platform for analysing the gene functions underlying oogenesis in addition to providing clues to the development of a similar culture system in other species.

Online Content Methods, along with any additional Extended Data display items and Source Data, are available in the online version of the paper; references unique to these sections appear only in the online paper.

Received 22 October 2015; accepted 22 September 2016.

Published online 17 October 2016.

- Surani, M. A., Hayashi, K. & Hajkova, P. Genetic and epigenetic regulators of pluripotency. *Cell* **128**, 747–762 (2007).
- Edson, M. A., Nagaraja, A. K. & Matzuk, M. M. The mammalian ovary from genesis to revelation. *Endocr. Rev.* **30**, 624–712 (2009).
- Hübner, K. *et al.* Derivation of oocytes from mouse embryonic stem cells. *Science* **300**, 1251–1256 (2003).
- Qing, T. *et al.* Induction of oocyte-like cells from mouse embryonic stem cells by co-culture with ovarian granulosa cells. *Differentiation* **75**, 902–911 (2007).
- Salvador, L. M., Silva, C. P., Kostetskii, I., Radice, G. L. & Strauss, J. F., III. The promoter of the oocyte-specific gene, *Gdf9*, is active in population of cultured mouse embryonic stem cells with an oocyte-like phenotype. *Methods* **45**, 172–181 (2008).
- Ohinata, Y. *et al.* Blimp1 is a critical determinant of the germ cell lineage in mice. *Nature* **436**, 207–213 (2005).
- McLaren, A. & Southee, D. Entry of mouse embryonic germ cells into meiosis. *Dev. Biol.* **187**, 107–113 (1997).
- Hayashi, K. *et al.* Offspring from oocytes derived from *in vitro* primordial germ cell-like cells in mice. *Science* **338**, 971–975 (2012).
- Morohaku, K. *et al.* Complete *in vitro* generation of fertile oocytes from mouse primordial germ cells. *Proc. Natl Acad. Sci. USA* **113**, 9021–9026 (2016).
- Ohinata, Y., Sano, M., Shigeta, M., Yamanaka, K. & Saitou, M. A comprehensive, non-invasive visualization of primordial germ cell development in mice by the *Prdm1-mVenus* and *Dppa3-ECFP* double transgenic reporter. *Reproduction* **136**, 503–514 (2008).
- Hayashi, K., Ohta, H., Kurimoto, K., Aramaki, S. & Saitou, M. Reconstitution of the mouse germ cell specification pathway in culture by pluripotent stem cells. *Cell* **146**, 519–532 (2011).
- McClellan, K. A., Gosden, R. & Takeo, T. Continuous loss of oocytes throughout meiotic prophase in the normal mouse ovary. *Dev. Biol.* **258**, 334–348 (2003).
- Lucifero, D., Mann, M. R., Bartolomei, M. S. & Trasler, J. M. Gene-specific timing and epigenetic memory in oocyte imprinting. *Hum. Mol. Genet.* **13**, 839–849 (2004).
- Peaston, A. E. *et al.* Retrotransposons regulate host genes in mouse oocytes and preimplantation embryos. *Dev. Cell* **7**, 597–606 (2004).
- Veselovska, L. *et al.* Deep sequencing and de novo assembly of the mouse oocyte transcriptome define the contribution of transcription to the DNA methylation landscape. *Genome Biol.* **16**, 209 (2015).
- Tanaka, S. *et al.* Placentomegaly in cloned mouse concepti caused by expansion of the spongiotrophoblast layer. *Biol. Reprod.* **65**, 1813–1821 (2001).

17. Ying, Q. L. *et al.* The ground state of embryonic stem cell self-renewal. *Nature* **453**, 519–523 (2008).
18. Irie, N. *et al.* SOX17 is a critical specifier of human primordial germ cell fate. *Cell* **160**, 253–268 (2015).
19. Sasaki, K. *et al.* Robust *in vitro* induction of human germ cell fate from pluripotent stem cells. *Cell Stem Cell* **17**, 178–194 (2015).

Supplementary Information is available in the online version of the paper.

Acknowledgements We thank Y. Takada for technical support, H. Ohta for technical advice on the iPSCs and embryo transfer, Y. Ohkawa for technical assistance on the RNA-seq, K. Kitajima and C. Meno for providing microscopes, F. Arai for providing FACS AriaII, and H. Leitch for proofreading the manuscript. We also thank the Research Support Center, Research Center for Human Disease Modeling, Kyushu University Graduate School of Medical Sciences for technical assistance. N.H. was a JSPS Research Fellow. This study was supported in part by a Grant-in-Aid from the Ministry of Education, Culture, Sports, Science, and Technology of Japan (KAKENHI #25114006); by JST-PRESTO; by the Uehara Memorial Foundation; and by the Takeda Science Foundation.

Author Contributions O.H., N.H., S.S. and K.H. performed the culture, embryo transfer, immunofluorescence, PCR analysis and chimaera analysis; O.H., N.H., S.S. and K.H. performed the differentiation to mature oocytes and are able to replicate the entire process, independently. N.H., T.I., and K.N. performed the RNA-seq analysis. G.N. generated the iPSC lines. Y.O. and Y.H. conducted the assessment of the culture conditions. M.S. contributed to the inception of the study. K.H. designed the experiments and wrote the manuscript.

Author Information The RNA-seq data have been deposited at Gene Expression Omnibus (GEO) database under accession number GSE79729. Reprints and permissions information is available at www.nature.com/reprints. The authors declare no competing financial interests. Readers are welcome to comment on the online version of the paper. Correspondence and requests for materials should be addressed to K.H. (hayashik@hgs.med.kyushu-u.ac.jp).

Reviewer Information *Nature* thanks D. Egli, S. Mitalipov and the other anonymous reviewer(s) for their contribution to the peer review of this work.

METHODS

A detailed protocol for oocyte production from pluripotent stem cells is available on the Nature Protocol Exchange at <http://dx.doi.org/10.1038/protex.2016.065>.

Data reporting. No statistical methods were used to predetermine sample size. The experiments were not randomized. The investigators were not blinded to allocation during experiments and outcome assessment.

Animals. All animal experiments were performed under the ethical guidelines of Kyushu University (the approval numbers A26-260-0 and A28-109-0). ICR, C57Bl/6J and 129X1/svj mice were purchased from Japan SLC. 129X1/svj females were mated with C57Bl/6J males to obtain hybrid mice (129X1/svj × C57Bl/6J). Pregnant females were killed by cervical dislocation to obtain E12.5 embryos. From female embryos, the gonads were isolated and then dissociated for rOvary formation²⁰.

ESCs and iPSCs. Two independent ESC lines bearing the BVSC reporter constructs, BVSCH18 and BVSCH14, were used in this study. Both ESC lines were established in our laboratory from the blastocysts collected from independent pairs of 129^{+Ter}/svj (agouti) females and C57BL/6 BVSC males⁸. These ESC lines were maintained under a 2i+LIF condition without feeders¹⁷.

For generation of iPSCs, MEFs and TTFs were obtained from E12.5 female embryos and 10-week-old female mice, respectively. Both embryos and mice were derived from mating between 129X1/svj (chinchilla) female and C57BL/6 BVSC males. Preparation of MEFs and TTFs and establishment of iPSCs in our laboratory were performed as described previously^{21,22} with slight modifications. Briefly, for MEF preparation, the embryos were minced, digested by trypsin-EDTA (Invitrogen), and then cultured in DMEM containing 10% FBS supplemented with 2 mM glutamine and 1 × penicillin/streptomycin (MEF medium). For TTF preparation, the tails were cut, their epidermises were removed and the remaining tails were minced into about 1 cm pieces. They were then cultured with MF-start medium (Toyobo) for 5 days. The cells migrating out from the tail were cultured in MEF medium.

MEFs and TTFs were reprogrammed to iPSCs by introducing retroviral vectors containing the four genes (pMXs-*Pou5f1*, pMXs-*Sox2*, pMXs-*Klf4* and pMXs-*c-Myc*). MEFs and TTFs were cultured in MEF medium for four days and then were reseeded on STO feeder cells. One day after the reseed, the medium was changed to Knockout DMEM (Invitrogen) supplemented with 15% KnockOut Serum Replacement (KSR; Invitrogen), 2 mM glutamine, 1 mM non-essential amino acids, 55 μM 2-mercaptoethanol, 10³ U ml⁻¹ leukaemia inhibitory factor (LIF), and 1 × penicillin/streptomycin. The medium was changed every other day. When ES-like colonies emerged, which usually took more than 14 days after infection, the medium was changed to 2i+LIF. ES-like colonies were picked up and propagated in 2i+LIF. These iPSC lines were maintained under a 2i+LIF condition without feeders. The ESC and iPSC lines in this study have not been tested for mycoplasma contamination.

Formation of reconstituted ovaries. PGCLCs were differentiated from ESCs or iPSCs as described previously²⁰, purified by FACSaria II (BD Bioscience) and aggregated with E12.5 female gonadal somatic cells in a low-binding U-bottom 96-well plate (NUNC) for 2 days of culture in GK15 supplemented with 1 μM retinoic acid. To strictly remove residual PGCs from dissociated gonadal cells, both SSEA1 and CD31 antibodies (Miltenyi Biotec) were used according to the manufacturer's instructions. 5,000 PGCLCs were cultured with 50,000 gonadal somatic cells to produce one reconstituted ovary.

IVDi culture. Reconstituted ovaries were placed on Transwell-COL membranes (Coaster) soaked in αMEM-based IVDi medium: αMEM supplemented with 2% FCS, 150 μM ascorbic acid (Sigma), 1 × Glutamax, 1 × penicillin/streptomycin and 55 μM 2-mercaptoethanol (Life Technologies). At 4 days of culture, the culture medium was changed to StemPro-34-based IVDi medium: StemPro-34 SFM (Life Technologies) supplemented with 10% FCS, 150 μM ascorbic acid, 1 × Glutamax, 1 × penicillin/streptomycin and 55 μM 2-mercaptoethanol. From 7 days to 10 days of culture, 500 nM ICI182780 was added to the StemPro-34-based IVDi medium. At 21 days of culture, individual 2FLs were manually dissociated using sharpened tungsten needles.

Isolation of 2FLs. Electrically sharpened tungsten needles were used for the isolation of individual 2FLs. Interstitial cells between 2FLs were carefully removed. The 2FLs were separated from the rOvary and placed at largely regular intervals.

IVG culture. The single 2FLs on the Transwell-COL membranes were soaked in IVG-αMEM medium: αMEM supplemented with 5% FCS, 2% polyvinylpyrrolidone (Sigma), 150 μM ascorbic acid, 1 × Glutamax, 1 × penicillin/streptomycin, 100 μM 2-mercaptoethanol, 55 μg ml⁻¹ sodium pyruvate (Nacalai Tesque), 0.1 IU ml⁻¹ follicle-stimulating hormone (Follistim; MSD), 15 ng ml⁻¹ BMP15 and 15 ng ml⁻¹ GDF9 (R&D Systems). At 2 days of culture, BMP15 and GDF9 were withdrawn from the medium and then follicles were incubated in 0.1% TypeIV Collagenase (MP Biomedicals). After washing with αMEM supplemented with 5%

FCS several times, the follicles were cultured in IVG-αMEM without BMP15 and GDF9. At 11 days of culture, cumulus-oocyte complexes grown on the membrane were picked up by a fine glass capillary.

IVM culture. Cumulus-oocyte complexes were transferred to IVM medium: αMEM supplemented with 5% FCS, 25 μg ml⁻¹ sodium pyruvate, 1 × penicillin/streptomycin, 0.1 IU ml⁻¹ follicular-stimulating hormone, 4 ng ml⁻¹ EGF, and 1.2 IU ml⁻¹ hCG (gonadotropin; ASKA). At 16h of culture, swollen cumulus cells were stripped from the oocytes by treating with hyaluronidase (Sigma), and then MII oocytes were determined by 1st polar body extrusion. Due to concerns of damages from a short-wavelength light (405 nm) for detection of SC, a small number of SC-negative oocytes (an estimated 5% of total oocytes) were not removed but subjected simultaneously to the following IVF experiments. For experiments that need to purify SC-positive oocytes, such as analyses of the diameters, imprinting gene loci, the chromosome number and transcriptome, SC-positive oocytes were carefully collected under a fluorescent microscopy with the short-wavelength light. The contamination rate of the endogenous ICR MII oocytes resulted from the selection in these experiments.

IVF and embryo transfer. MII oocytes were subjected to IVF as described previously and then fertilized eggs were cultured in HTF medium (ARK Resource). 2-cell embryos were transferred into the oviduct of 0.5 days post coitum (d.p.c.) pseudopregnant ICR females. Some of the 2-cell embryos were cultured in KSOM (ARK Resource) for 4 days until the blastocyst stage. Newborns were delivered from the mother by Caesarean section and nursed by surrogate ICR mothers.

RNA-seq analysis. A directional RNA-seq library was constructed as described previously²³. Briefly, poly(A)⁺ RNAs were purified from 100–15,000 cells or oocytes (ESCs, 10,000–13,200; PGCLC-d6, 10,000; PGCLC-agg3, 5,300–15,000; vitro-2nd and vivo-2nd: 337–12; vitro-MII and vivo-MII: 99–134), using a Dynabeads mRNA DIRECT Micro Kit (Invitrogen). For vitro-2nd and vitro-MII, SC-positive oocytes were collected under a fluorescence microscopy. Biologically triplicated samples were prepared in each stage. Purified RNAs were subjected to library construction using a NEBNext Ultra Directional RNA Library Prep Kit for Illumina (NEB). cDNAs were enriched by 12-cycle PCR. Sequencing of the libraries was performed with HiSeq2000 (Illumina). Obtained reads were processed with the FASTX tool kit²⁴ to remove short (<20 bp) and low quality (quality score <20) reads, followed by trimming of the adaptor sequence. Processed reads were mapped to the mouse mm10 genome using TopHat2/Bowtie2²⁵. Cuffdiff²⁶, a program in the Cufflinks software, and QuasR²⁷, a Bioconductor package, were used for the differential gene and repetitive sequence expression analyses. Hierarchical clustering and principal component analysis were performed with R, based on RefSeq gene expression levels.

Generation of rESCs. Derivation of rESCs was performed using 2i+LIF¹⁷ medium. Briefly, fertilized eggs derived from *in-vitro*-generated oocytes were cultured in KSOM until the blastocyst stage. The blastocysts were placed on MMC-treated mouse embryonic fibroblasts and cultured in 2i+LIF. After 5 to 7 days of culture, colonies were picked up and passaged several times to establish rESCs. During establishment, rESCs were passaged on a culture plate coated with 300 ng ml⁻¹ laminin (BD Bioscience) to remove mouse embryonic fibroblasts.

Chimaera analysis. rESCs were injected into the wild-type blastocysts. The blastocysts were transferred into the uterus of 2.5 d.p.c. pseudopregnant females and the embryos were collected at 10 days after transplantation. The embryos and their gonads were observed under a fluorescent microscope (SZX16; Olympus). For analysis of the contribution of rESCs to various tissues, the neural tube, lung, heart, liver, intestine and tail were collected and subjected to PCR analyses.

Genotyping. Genomic DNAs isolated from the tails of offspring, rESC lines and fetal tissues were subjected to PCR amplification using the primers (Supplementary Table 2). For sexing, PCR reaction amplified a 253 bp fragment from the X chromosome and 355 bp and 399 bp fragments from the Y chromosome. PCR products were resolved through electrophoresis in agarose gels and illuminated by ethidium bromide (EtBr).

COBRA analysis and bisulfite sequencing. Genomic DNAs were isolated from more than 200 SC-positive MII oocytes generated *in vitro* and wild-type MII oocytes *in vivo*, and from tails of offspring from *in-vitro*-derived oocytes and wild-type mice. Bisulfite reactions were performed using a Methylamp DNA Modification Kit (Epigentek). For COBRA analysis, the DMRs of *H19*, *Igf2r*, *Peg3* and *Snrpn* were amplified with specific primers (Supplementary Table 2), as described previously^{28,29}. The amplified DNA was digested with the following restriction enzymes (NEB): PvuI-HF for *H19*, HpyCH4IV for *Igf2r* and *Peg3*, and AciI for *Snrpn*. The digested samples were resolved through electrophoresis in 2% or 3% agarose gels and illuminated by EtBr. The PCR products were subcloned into the pGEM-T Easy vector (Promega) and were sequenced. For bisulfite sequencing of genomic DNA from oocytes, PCR amplification of the DMRs of *H19* and *Igf2r* was carried out as described previously¹³. The PCR products were subcloned into

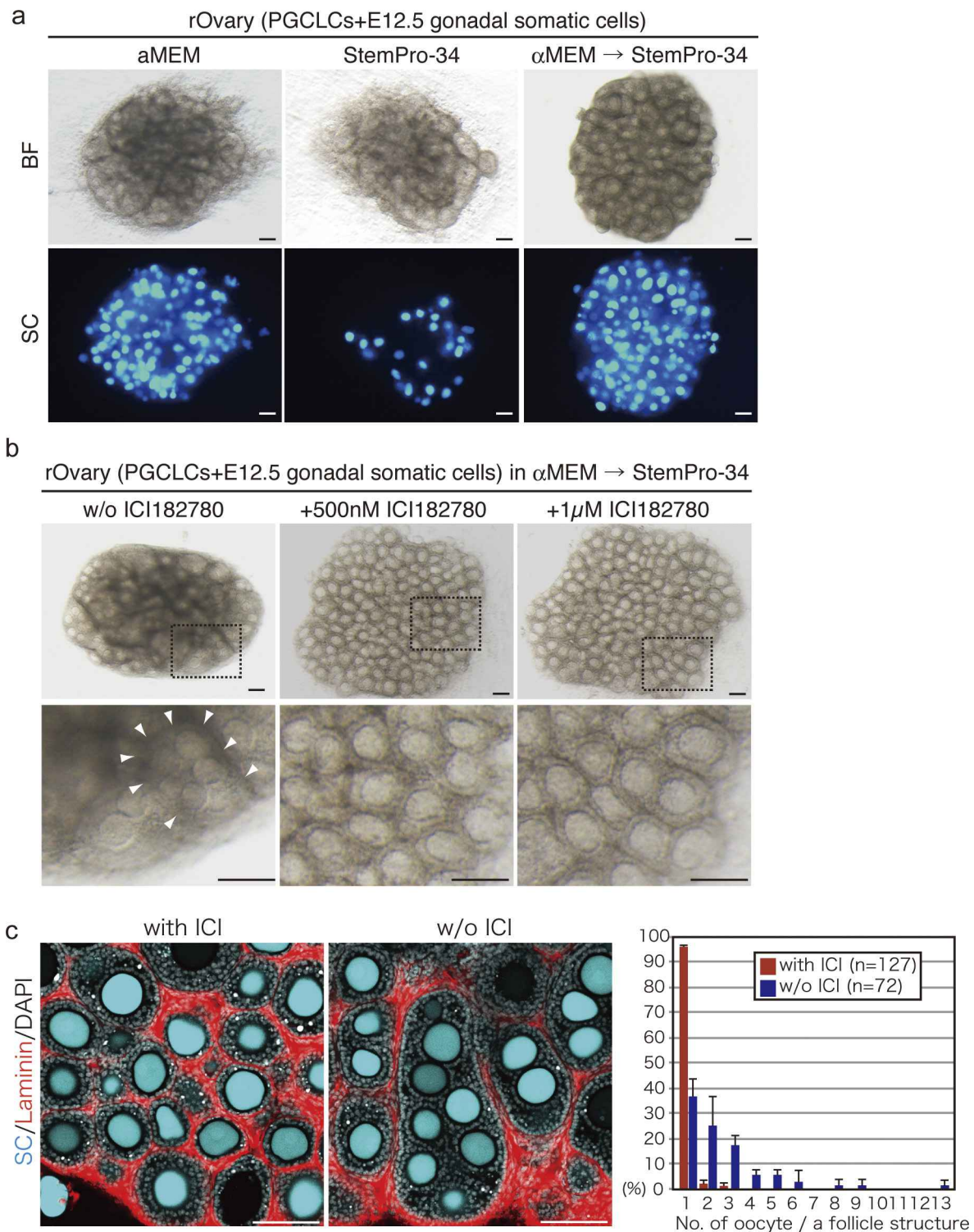
the pGEM-T Easy vector (Promega) and were sequenced. The sequences were analysed and aligned by QUMA software³⁰.

Immunofluorescence analysis. For whole-mount immunofluorescence analysis, rOvaries were fixed in 4% paraformaldehyde for 1 h at room temperature, washed three times in PBST (PBS containing 0.2% Triton X-100), soaked in blocking buffer (PBS containing 0.1% BSA and 0.3% Triton X-100) overnight at 4 °C, and then incubated with primary antibodies (anti-GFP rat monoclonal antibody (mAb) (Nakalai 04404-84) cross-reactive to BV and SC, and anti-Foxl2 goat polyclonal antibody (pAb) (Novus Biologicals NB100-1277) or anti-laminin rabbit pAb (Abcam ab11575)) in the blocking buffer overnight at 4 °C. After washing five times in PBST, the rOvaries were incubated with secondary antibodies (anti-rat IgG donkey pAb Alexa488 and anti-goat IgG donkey pAb Alexa568 or anti-rabbit IgG donkey pAb Alexa568) and DAPI in the blocking buffer overnight at 4 °C. The rOvaries were washed five times in PBST and mounted in Fluo-KEEPER antifade reagent (Nakalai).

Immunofluorescence of the chromosome in meiotic prophase I was performed as described previously³¹ with slight modifications. Briefly, for the chromosome in meiotic prophase I, rOvaries were dissociated by incubation in CTK (0.1 mg ml⁻¹ collagenase IV, 0.25% Trypsin, 20% KSR and 1 mM CaCl₂ in PBS) for 30 min at 37 °C, followed by Accutase (Nakalai) for 5 min at 37 °C. Dissociated single cells were suspended in hypotonic buffer and placed on glass slides. Slides were washed three times in PBS, soaked in blocking buffer (PBS containing 10% FBS) for 1 h at room temperature and then incubated with primary antibodies (anti-SCP1 rabbit pAb (Novus Biologicals NB300-ss9) and anti-SCP3 mouse mAb (Abcam ab97672)) overnight at 4 °C. After washing three times in PBS containing 0.05% Tween20, the slides were incubated with secondary antibodies (anti-rabbit IgG goat pAb Alexa568 and anti-mouse IgG donkey pAb Alexa647), washed three times in PBS containing 0.05% Tween20, and then incubated with anti-γH2AXSer139 mouse mAb directly conjugated with FITC (Millipore 16-202A) and DAPI. The slides were washed three times in PBS containing 0.05% Tween20 and mounted in Fluo-KEEPER antifade reagent (Nakalai). Immunofluorescence of the chromosome in MII oocytes was performed as described previously³². The primary antibodies

used were anti-centromere human pAb (Antibodies Incorporated 15-235-001) and anti-H3K9me3 rabbit pAb (Millipore 07-442). The secondary antibodies used were anti-human IgG donkey pAb Alexa488 and anti-rabbit IgG goat pAb Alexa568. All immunofluorescence samples were analysed by a confocal microscope (Zeiss LSM700).

20. Hayashi, K. & Saitou, M. Generation of eggs from mouse embryonic stem cells and induced pluripotent stem cells. *Nat. Protocols* **8**, 1513–1524 (2013).
21. Takahashi, K. & Yamanaka, S. Induction of pluripotent stem cells from mouse embryonic and adult fibroblast cultures by defined factors. *Cell* **126**, 663–676 (2006).
22. Nagamatsu, G. *et al.* A germ cell-specific gene, *Prmt5*, works in somatic cell reprogramming. *J. Biol. Chem.* **286**, 10641–10648 (2011).
23. Hamazaki, N., Uesaka, M., Nakashima, K., Agata, K. & Imamura, T. Gene activation-associated long noncoding RNAs function in mouse preimplantation development. *Development* **142**, 910–920 (2015).
24. Patel, R. K. & Jain, M. NGS QC Toolkit: a toolkit for quality control of next generation sequencing data. *PLoS One* **7**, e30619 (2012).
25. Kim, D. *et al.* TopHat2: accurate alignment of transcriptomes in the presence of insertions, deletions and gene fusions. *Genome Biol.* **14**, R36 (2013).
26. Trapnell, C. *et al.* Differential gene and transcript expression analysis of RNA-seq experiments with TopHat and Cufflinks. *Nat. Protocols* **7**, 562–578 (2012).
27. Gaidatzis, D., Lerch, A., Hahne, F. & Stadler, M. B. QuasR: quantification and annotation of short reads in R. *Bioinformatics* **31**, 1130–1132 (2015).
28. Li, X. *et al.* A maternal-zygotic effect gene, *Zfp57*, maintains both maternal and paternal imprints. *Dev. Cell* **15**, 547–557 (2008).
29. Lee, J. *et al.* Erasing genomic imprinting memory in mouse clone embryos produced from day 11.5 primordial germ cells. *Development* **129**, 1807–1817 (2002).
30. Kumaki, Y., Oda, M. & Okano, M. QUMA: quantification tool for methylation analysis. *Nucleic Acids Res.* **36**, W170–W175 (2008).
31. Takada, Y. *et al.* HP1 γ links histone methylation marks to meiotic synapsis in mice. *Development* **138**, 4207–4217 (2011).
32. Hodges, C. A. & Hunt, P. A. Simultaneous analysis of chromosomes and chromosome-associated proteins in mammalian oocytes and embryos. *Chromosoma* **111**, 165–169 (2002).



Extended Data Figure 1 | Evaluation of the basal culture conditions.

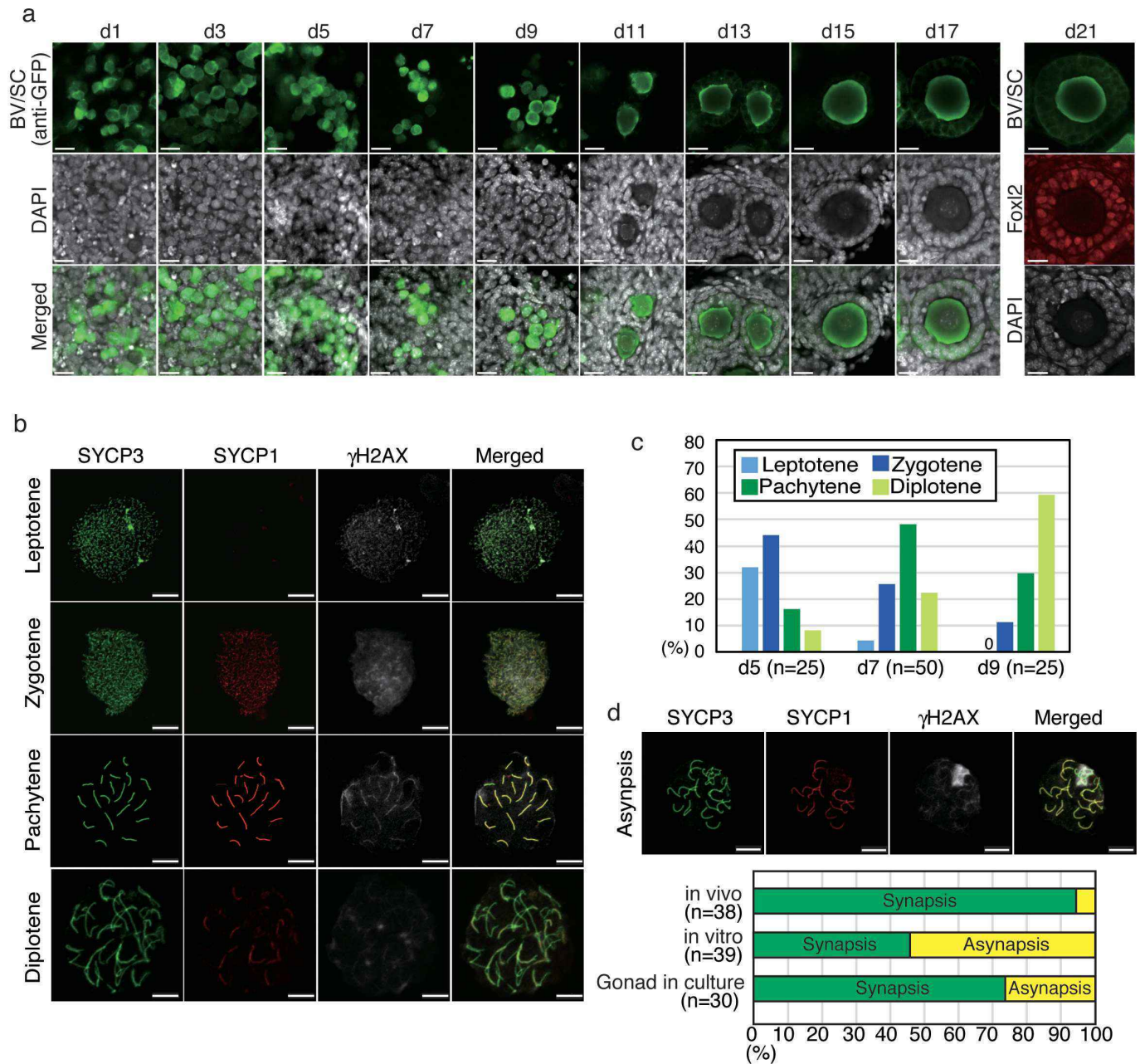
a, Culture of rOvaries. Representative images of rOvaries at 3 weeks of culture in the medium indicated on the top are shown. Note that a number of SC-positive oocytes were formed with firm structure of rOvary under the combined culture condition. BF, bright field; SC, *stella-ECFP*.

b, Culture of rOvaries with ICI182780, an oestrogen inhibitor.

Representative images of rOvaries under the culture condition indicated on the top are shown. The images on the bottom of the figure are high-magnification images of the region in the dashed box. Note that multiple oocyte follicles (white arrowheads) were frequently observed in the

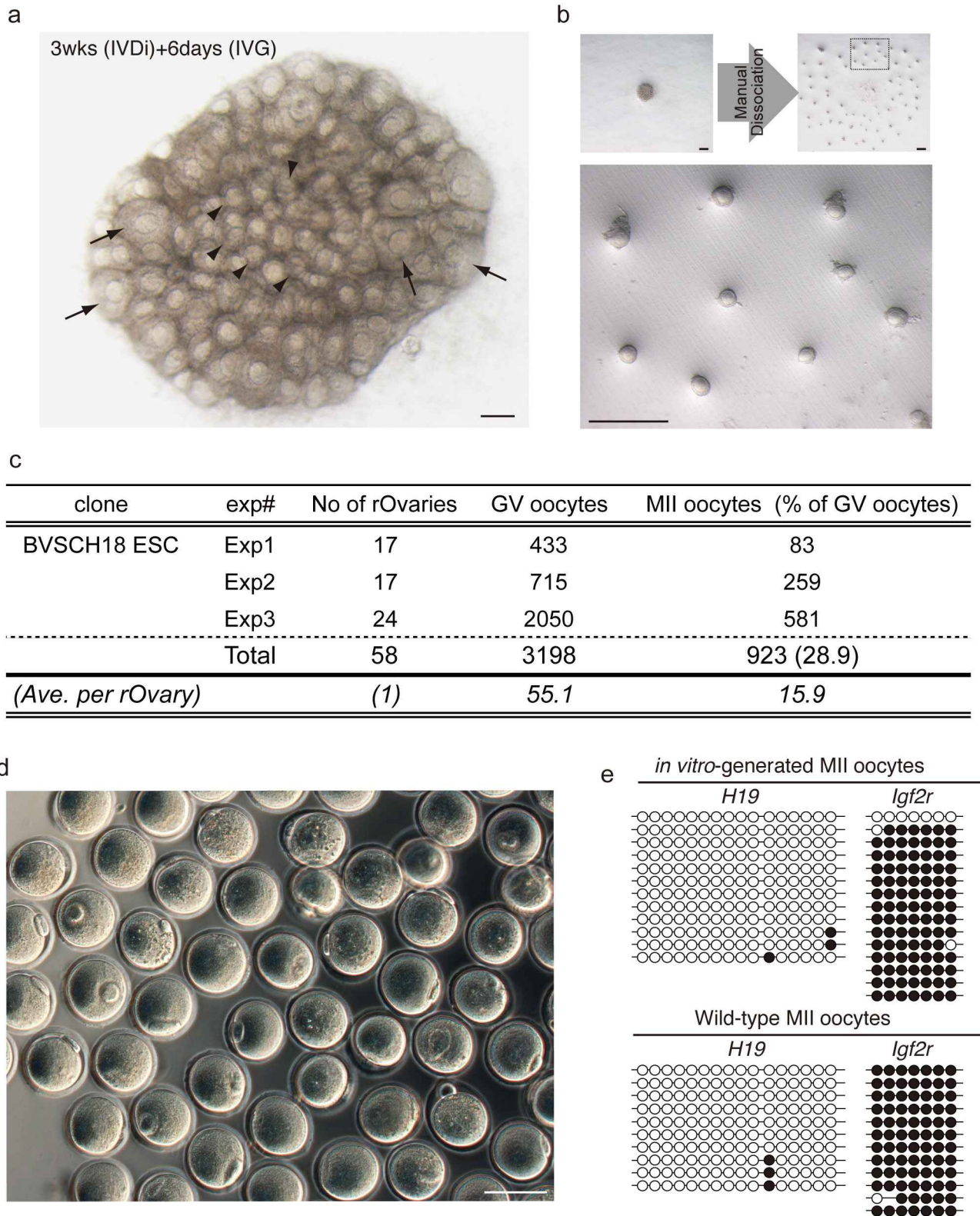
culture without ICI182780 but were rarely observed in the culture with the inhibitor. **c**, Immunofluorescence analysis of the follicle structure. Images are rOvaries at 3 weeks of culture with or without ICI182780.

Immunostaining with laminin, a component of the basement membrane, was used to define the follicle structure that encloses oocyte(s). The bar graph on the right shows the percentage of follicles with single or multiple oocytes. The mean values \pm s.d. from 3 biological replicates are shown. The total numbers of follicles counted are shown in the box. Scale bars, 100 μ m.



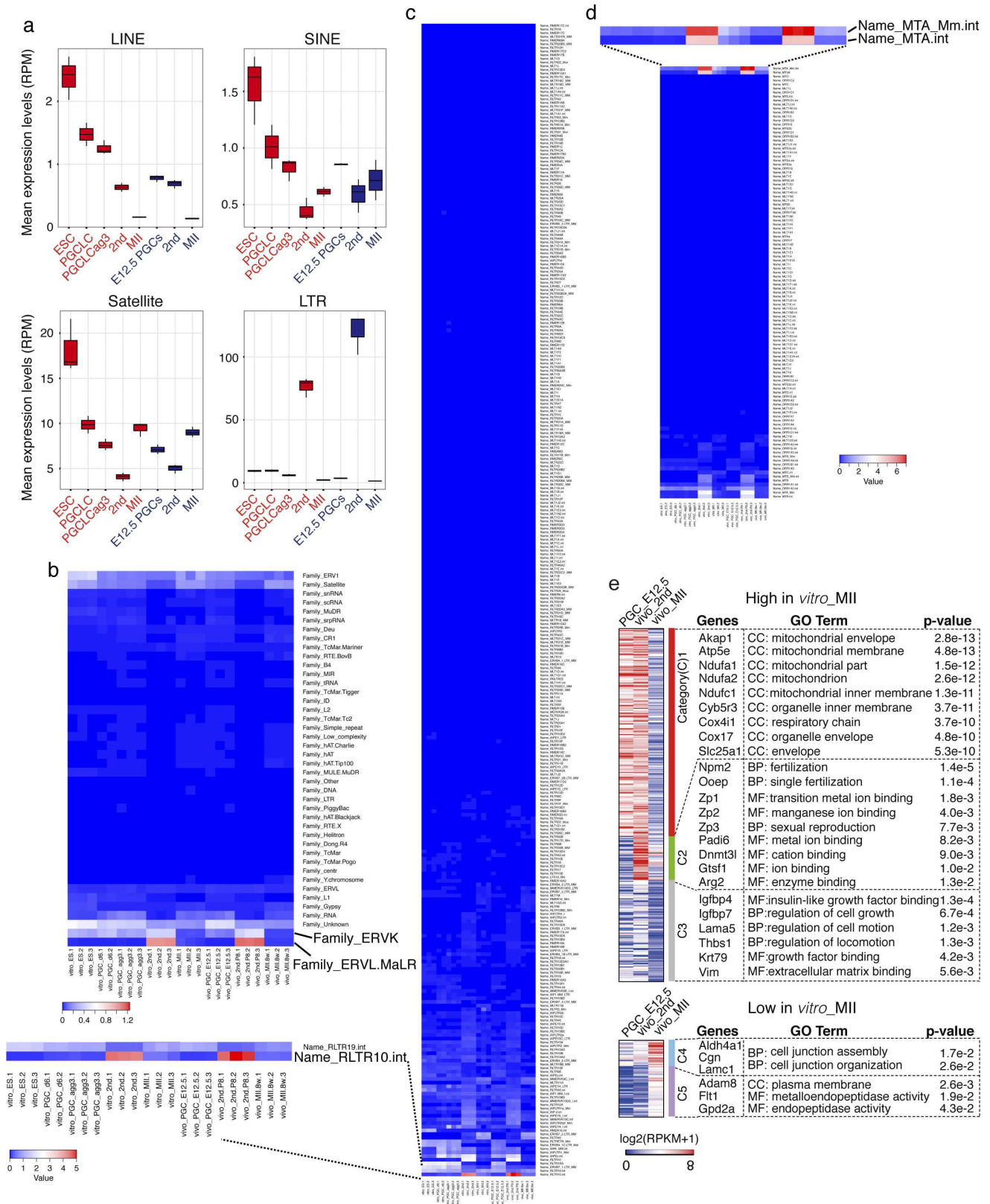
Extended Data Figure 2 | Meiotic progression and establishment of genomic imprints in culture. **a**, PGC-to-oocyte differentiation during IVDi. PGCLCs and oocytes were visualized by anti-GFP antibody (green) cross-reactive to BV and SC. At 21 days of culture, cells surrounding the oocyte expressed Foxl2 (red). Scale bars, 20 μ m. **b**, Representative images of each stage of meiotic prophase I in culture. Meiotic cells from the culture were spread and stained with the antibodies indicated. The colours were converted by ZEN software (Zeiss). **c**, Meiotic progression in IVDi culture. Percentages of each stage in total meiotic cells are shown.

The meiotic cells in the rOvaries were obtained from 3 independent experiments. **d**, Asynapsis of meiotic chromosome at the pachytene stage in culture. Representative immunofluorescence images of asynapsis at the pachytene stage are shown. Note that γ H2AX is densely accumulated in the meiotic chromosome. The graph below the images shows the percentage of asynapsis in cells at the pachytene stages in three E17.5 female gonads, four rOvaries or three E12.5 gonads cultured for 5 days, from 3 independent experiments. Scale bars in **b** and **d**, 10 μ m.



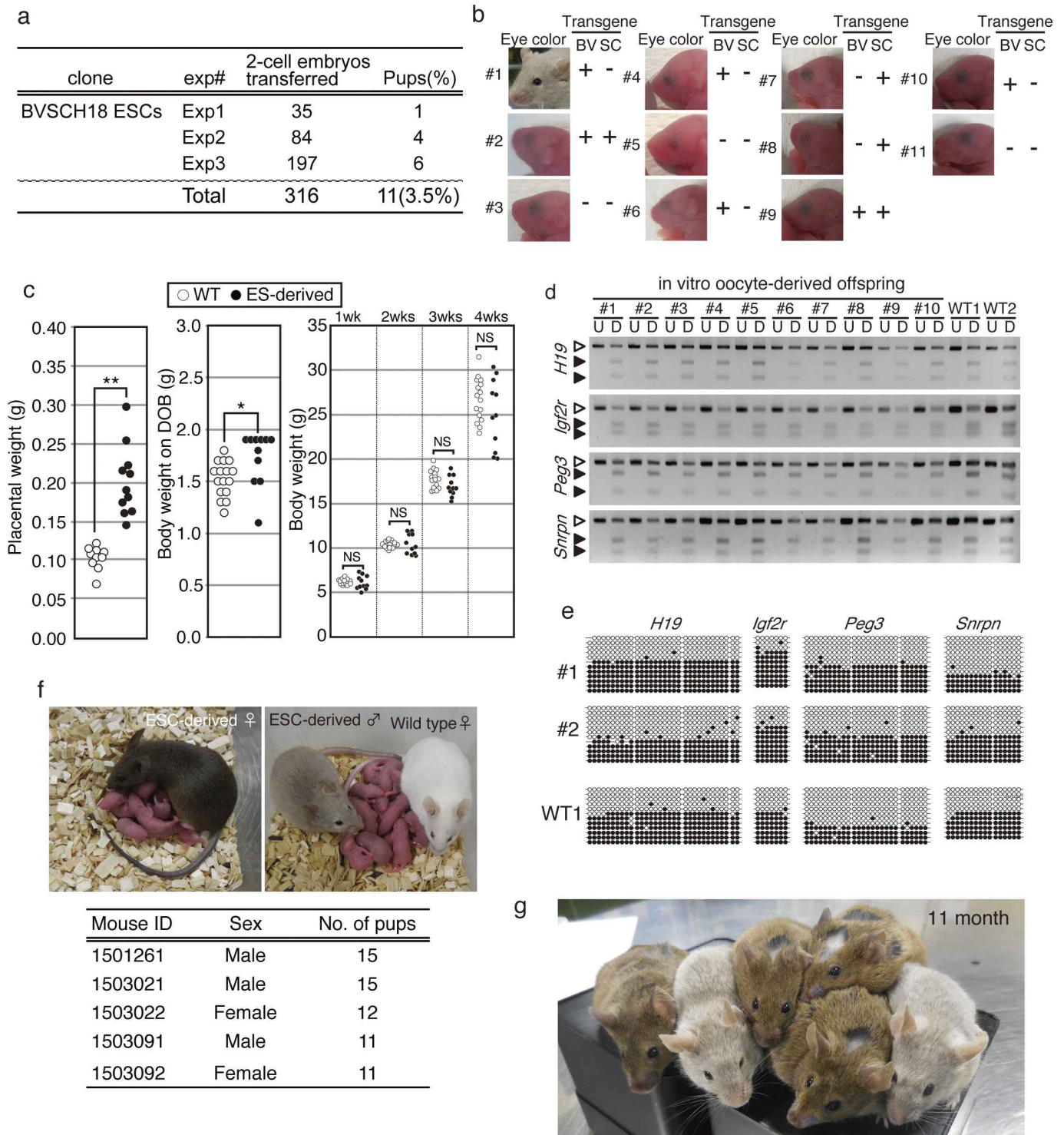
Extended Data Figure 3 | Isolation of individual 2FLs for IVG culture and MII oocytes from IVM culture. **a**, Attenuated maturation in an intact rOvary. Cell proliferation in the granulosa cell layer is observed only in 2FLs located at the edge of the rOvary (arrows). 2FLs in the middle seldom show cell proliferation in the granulosa cell layer (arrowheads). **b**, Representative images of isolation of individual 2FLs. A rOvary (left, upper) was mechanically dissociated (right upper). The high-magnification image of the boxed region shows individual 2FLs

after dissociation. **c**, The number of germinal vesicle and MII oocytes derived from BVSCH18 ESCs. The number of oocytes obtained from each experiment and the total number from all experiments were shown. **d**, A large image of the MII oocytes shown in Fig. 1d. **e**, Bisulfite sequence analysis of differentially methylated regions (DMRs) of the imprinted genes (*H19* and *Igf2r*) in MII oocytes generated *in vitro* and *in vivo*. White and black circles represent unmethylated and methylated CpG sequences, respectively. Scale bars, 100 μ m (**a**, **d**), 500 μ m (**b**).



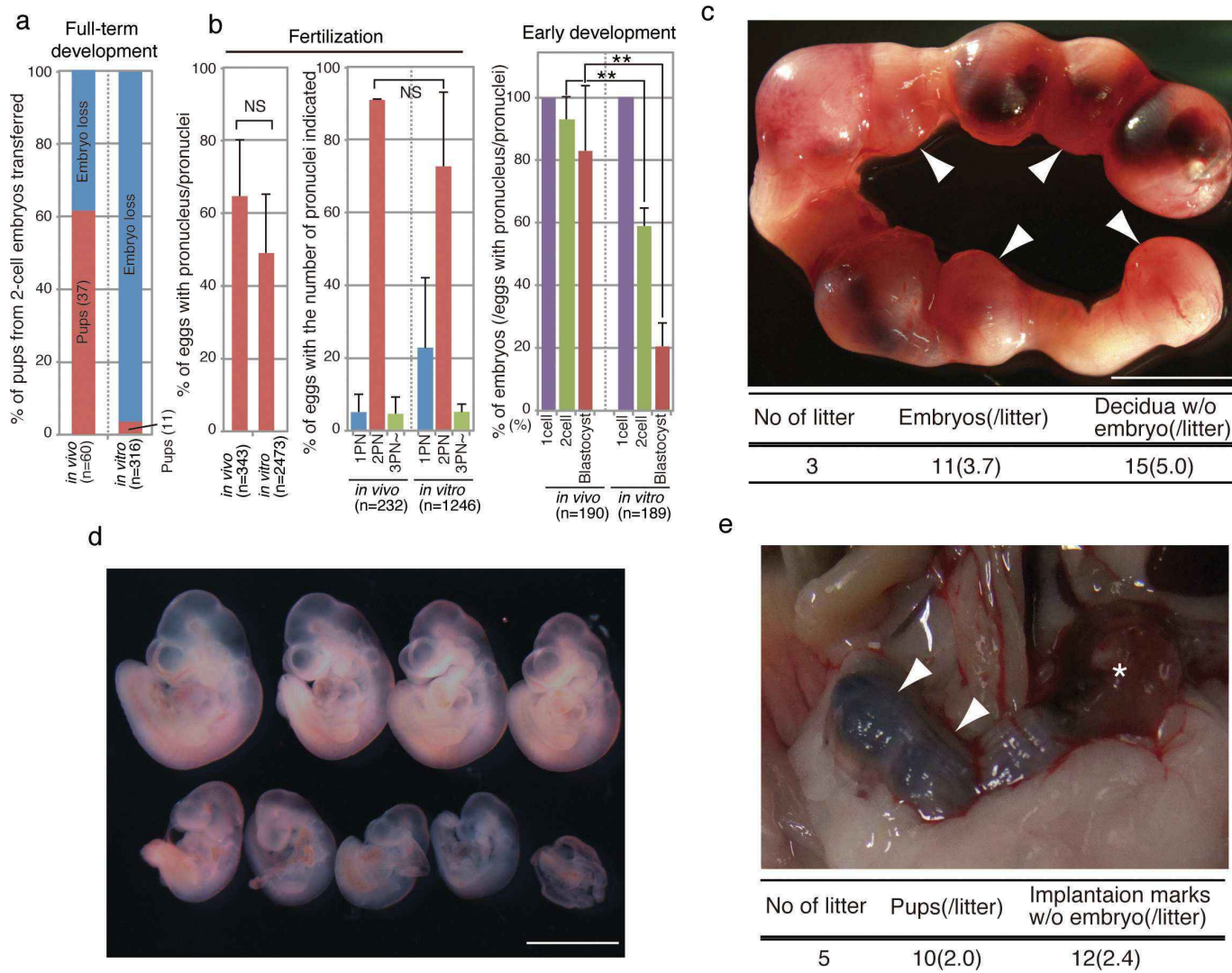
Extended Data Figure 4 | Expression of a specific class of LTR. **a**, Box plots showing the expression of repetitive elements. Reads per million mapped reads (RPMs) of each product are shown. Note that LTR products increased sharply in oocytes at the secondary follicle stage. **b**, **c**, **d**, Heat map of the normalized expression profile of the LTR family (**b**), ERVK

(**c**) and ERVL-MaLR (**d**). **e**, The gene ontology enrichments of genes categorized by their gene expression dynamics. All genes listed are shown in Supplementary Table 1. All expression data are based on the mean values from 3 biological replicates except for PGCLC(**d**) that is from 2 biological replicates.



Extended Data Figure 5 | Growth and fertility of offspring from *in-vitro*-generated oocytes. **a**, The number of 2-cell embryos and pups derived from BVSCH18 ESCs. **b**, Summary of eye colour and transgene of the pups (or adult mouse) derived from *in-vitro*-generated oocytes from BVSCH18 ESCs. **c**, Weights of placentas (left), newborn pups (middle) and development of the body weights (right) of offspring from the MII oocytes from BVSCH18 (closed circles) and the genetically matched wild-type mice (129X1/svjC57BL/6F1 × ICR) (closed circles) in 3 independent experiments (*t*-test, ***P* < 0.01, **P* < 0.05) **d**, Combined bisulfite restriction analysis (COBRA) of DMRs of the imprinted genes (*H19*, *Igf2r*, *Peg3* and *Snrpn*) in the 10 mice (1–10) derived from *in-vitro*-

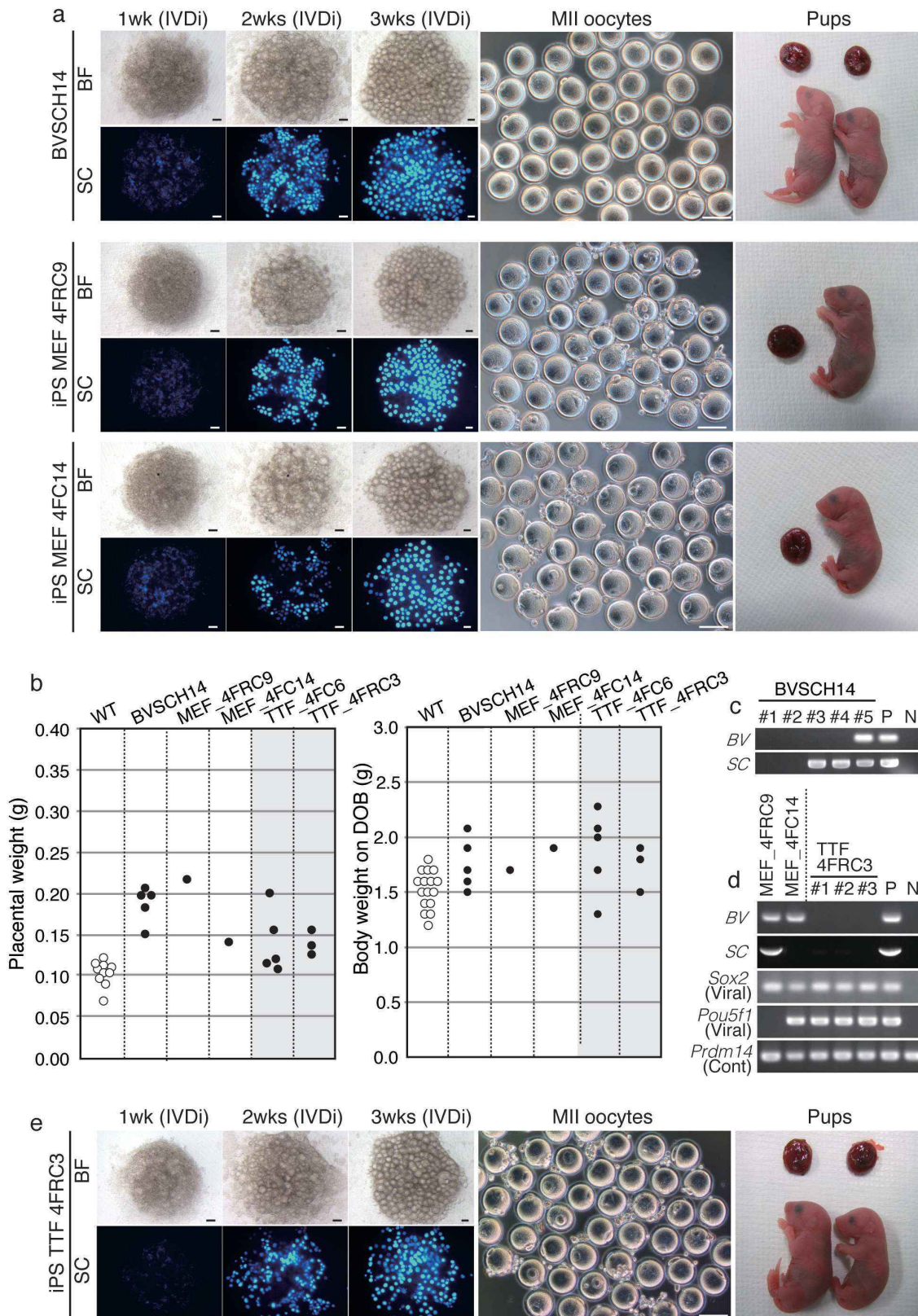
generated MII oocytes and the two wild-type mice (WT1 and WT2). PCR products were either digested (D) or undigested (U) with the respective enzyme. The digested and undigested fragments are indicated by black and white triangles, respectively. **e**, Bisulfite sequence analysis of DMRs of the imprinted genes in the two mice (1 and 2) from *in-vitro*-generated oocytes and the wild-type mouse (WT1). White and black circles represent unmethylated and methylated CpG sequences, respectively. **f**, A female (left) and a male (right) mouse from *in-vitro*-generated oocytes with full fertility. The table below the images shows the number of pups in a litter. **g**, The 6 mice derived from *in-vitro*-generated MII oocytes at 11 months after birth. For gel source data see Supplementary Fig. 1.



Extended Data Figure 6 | Developmental potential of *in-vitro*-generated oocytes.

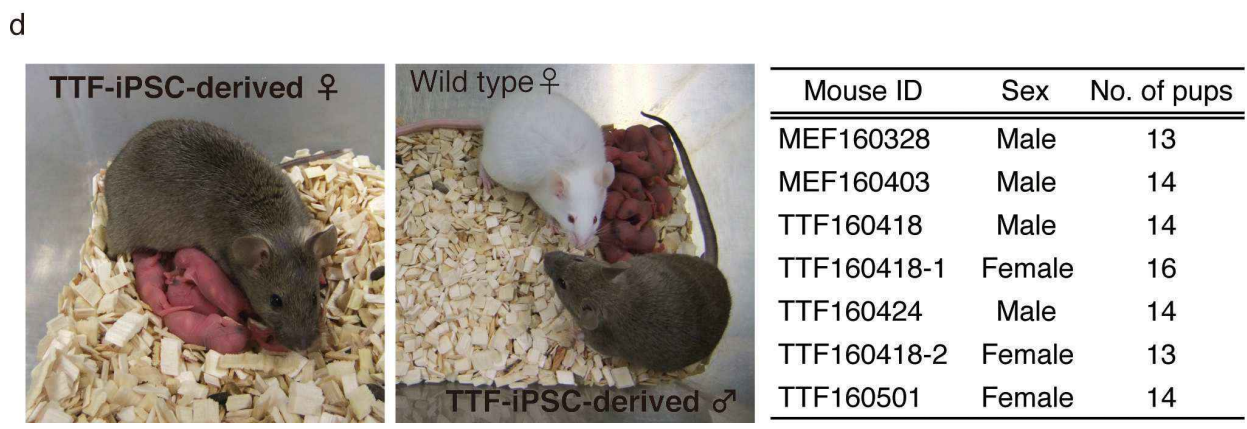
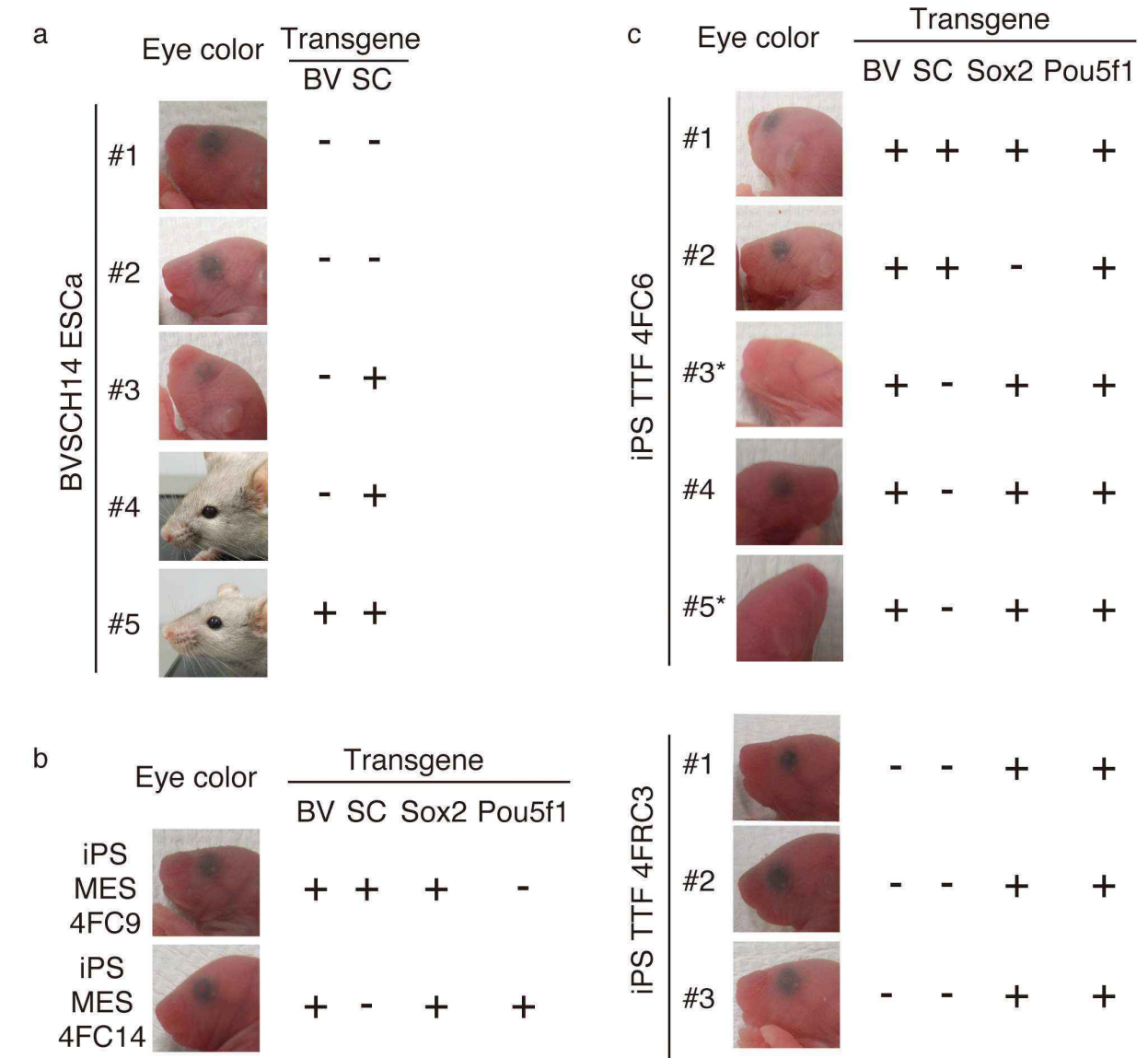
a, Percentages of pups from 2-cell embryos transferred. The numbers of pups obtained from 3 independent embryo transfer experiments are shown. **b**, Fertilization and preimplantation development. Eggs with pronucleus/pronuclei (PN) (left), the number of PN (middle) and early embryonic development in culture (right). The mean values \pm s.d. from 5 biological replicates are shown. The total numbers of oocytes/embryos are shown in each graph. **c**, A uterus at 10 days after transfer of embryos from ESC-derived oocytes. White arrowheads indicate degenerating conceptuses that had decidua without any apparent embryo, and therefore embryo loss at early gestation. The table below the image summarizes the numbers of remaining embryos and decidua

without embryo observed at 10 days of gestation. On average, 3.7 embryos remained in the uterus. Scale bar, 5 mm. **d**, Embryos collected from a day 10 uterus after transfer of embryos from ESC-derived oocytes. The developmental stage of the embryos was varied. Scale bar, 2 mm. **e**, Implantation marks in the uterus on Caesarean section. White arrowheads indicate the implantation marks without embryos and the asterisk shows the uterus wall after delivering newborn pups by Caesarean section. The table below the image summarizes the numbers of pups and implantation marks without embryos on Caesarean section. On average, 2 pups were obtained per uterus, indicating there was some amount of embryo loss during late gestation.



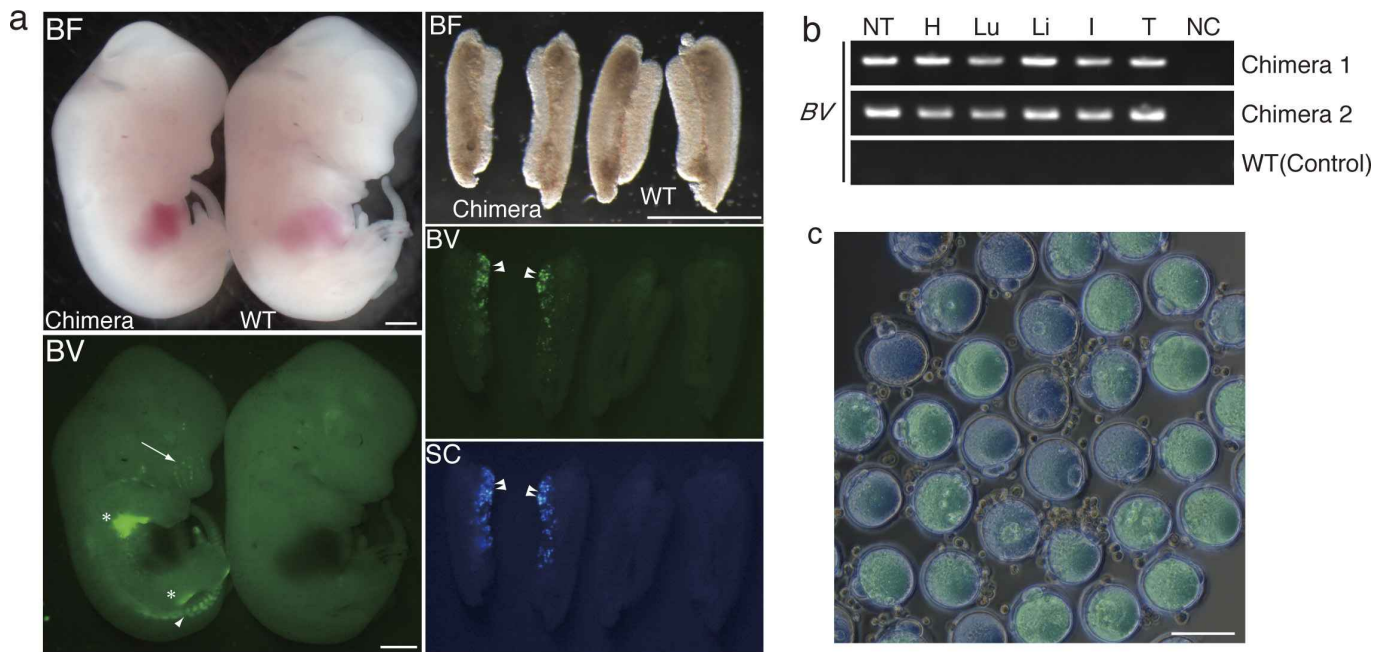
Extended Data Figure 7 | Oogenesis *in vitro* using other ESC and iPSC lines. **a**, Representative images of a rOvary in IVDi, MII oocytes and pups obtained from BVSCH14 ESCs and MEF-derived iPSC lines (MEF4FC9 and MEF4FC14). **b**, Weights of placentas (left) and newborns (right) from the MII oocytes from ESC/iPSC lines indicated on the top. The values are from 2 independent experiments (see also Extended Data Table 1). The values of the control are same as those shown in Extended Data

Fig. 5c, d, Genotyping of the pups from BVSCH14 ESCs (**c**) and iPSCs (**d**). PCR products from each gene indicated are shown. P, a positive control; N, a negative control. Details of the positive control and negative control are described in Fig. 3 legend. **e**, Representative images of a rOvary in IVDi using TTF-derived iPSCs (TTF4FC3), MII oocytes and pups obtained from TTF4FC3. Scale bars, 100 μ m. For gel source data see Supplementary Fig. 1.



Extended Data Figure 8 | Summary of eye colour and transgene of the pups derived from *in-vitro*-generated oocytes. a–c, A compiled list of eye colour and transgene of the pups derived from *in-vitro*-generated oocytes from BVSCH14 ESCs (a), MEF-derived iPSCs (MEF4FRC9 and MEF4FC14) (b), and TTF-derived iPSCs (TTF4FC6 and TTF4FRC3) (c). 3* and 5* pups from TTF4FC6 had albino eyes. This is because MEF-iPSCs and TTF-iPSCs (129X1/svj (chinchilla) × C57BL/6) used in this

study have Cc or Cc^{ch} genotype that effects eye pigmentation (see also Method). As ICR strain has cc genotype, half of the offspring would have albino eyes. Note that these pups had BV and the retroviral transgenes. d, Fertility of adult mice derived from *in-vitro*-generated oocytes from iPSCs. Both a female (left) and a male (middle) from TTF-derived iPSCs were fertile. The table (right) shows the number of pups in a litter.



Extended Data Figure 9 | Chimaera analysis of rESCs. **a**, Bright field (BF) and fluorescent image (BV or SC) of a representative chimaera and wild-type E12.5 embryos (left images), and their gonads with mesonephros (right images). BV expression was detectable in the sensory vibrissae (arrow), the mesenchyme of the forelimb and the hind limb (asterisks) and the myotome (arrowheads), as reported previously¹⁰. BV and SC expressions were detectable in PGCs in the gonads (double

arrowheads). Scale bars, 1 mm. **b**, BV transgene in chimaera embryos. PCR products from each tissue (NT, neural tube; H, heart; Lu, lung; Li, liver; I, intestine; T, tail; NC, a negative control from the genomic DNA of a wild-type embryo) are shown. **c**, MII oocytes from rESCs. The image in Fig. 4d merged with SC is shown. Scale bars, 100 μ m. **d**, A schematic drawing showing the *in vitro* reconstitution of the entire female germ line. For gel source data see Supplementary Fig. 1.

Extended Data Table 1 | Summary of oogenesis *in vitro* using BVSC14 ESCs and iPSCs derived from MEFs and TTFs

| clone | exp# | agg | GV oocyte (/rOvary) | MII oocyte (/rOvary) | Egg with PN (1PN, 2PN, 3PN) | 2cell embryos (% of Egg with PN) | 2cell embryos transferred ^a | pups (% of 2cell embryos transferred) |
|---------------|-------|-----|---------------------|----------------------|-----------------------------|----------------------------------|--|---------------------------------------|
| BVSC14 ESCs | Exp1 | 16 | 1616 | 683 | 438 (28, 385, 25) | 296 | 296 | 3 |
| | Exp2 | 29 | 2465 | 802 | 400 (65, 310, 25) | 267 | 133 | 2 |
| | Total | 45 | 4081 (90.7) | 1485 (33.0) | 838 (93, 695, 50) | 563 (67.2) | 429 | 5 (1.2) |
| iPS MEF_4FRC9 | Exp1 | 35 | 2939 | 841 | 410 (51, 320, 39) | 125 | 125 | 0 |
| | Exp2 | 31 | 2620 | 710 | 381 (86, 278, 17) | 241 | 241 | 1 |
| | Total | 66 | 5559 (84.2) | 1551 (23.5) | 791 (137, 598, 56) | 366 (46.3) | 366 | 1 (0.3) |
| iPS MEF_4FC14 | Exp1 | 33 | 2691 | 727 | 404 (41, 330, 33) | 104 | 94 | 0 |
| | Exp2 | 31 | 2397 | 902 | 319 (102, 210, 7) | 200 | 200 | 1 |
| | Total | 64 | 5088 (79.5) | 1629 (25.5) | 723 (143, 540, 40) | 304 (42.0) | 294 | 1 (0.3) |
| iPS TTF_4FC6 | Exp1 | 32 | 3185 | 658 | 576 (71, 465, 40) | 317 | 237 | 3 |
| | Exp2 | 31 | 3123 | 1042 | 540 (124, 364, 52) | 335 | 335 | 2 |
| | Total | 63 | 6308 (100.1) | 1700 (27.0) | 1116 (195, 829, 92) | 652 (58.4) | 572 | 5 (0.9) |
| iPS TTF_4FRC3 | Exp1 | 30 | 3765 | 1138 | 877 (176, 606, 95) | 335 | 335 | 1 |
| | Exp2 | 31 | N.C. ^b | 1210 | 711 (166, 501, 44) | 441 | 441 | 2 |
| | Total | 61 | 3765 (125.5) | 2348 (38.5) | 1588 (342, 1107, 139) | 776 (48.9) | 776 | 3 (0.4) |

^aAs they were used for other experiments, not all 2-cell embryos were transferred into the surrogate mothers.

^bNot counted.